

## Unexpected Imidazoquinoxalinone Annulation Products in the Photoinitiated Reaction of Substituted-3-Methyl-Quinoxalin-2-Ones with *N*-Phenylglycine<sup>†</sup>

Julio R. De la Fuente<sup>1\*</sup>, Álvaro Cañete<sup>2</sup>, Carolina Jullian<sup>1</sup>, Claudio Saitz<sup>1</sup> and Christian Aliaga<sup>3</sup>

<sup>1</sup>Departamento de Química Orgánica y Físicoquímica, Facultad de Ciencias Químicas y Farmacéuticas, Universidad de Chile, Santiago, Chile

<sup>2</sup>Departamento de Química Orgánica, Facultad de Química, Pontificia Universidad Católica de Chile, Santiago, Chile

<sup>3</sup>Departamento de Ciencias del Ambiente, Facultad de Química y Biología, Universidad de Santiago de Chile, Santiago, Chile

Received 15 May 2013, accepted 19 August 2013, DOI: 10.1111/php.12162

### ABSTRACT

Photoinduced electron transfer between *N*-phenylglycine (NPG) and electronically excited triplets of 7-substituted-3-methyl-quinoxalin-2-ones in acetonitrile generate the respective ion radical pair, where by decarboxylation the phenyl-amino-alkyl radical, PhNHCH<sub>2</sub>•, is generated. This radical reacts with the 3-methyl-quinoxalin-2-ones ground states, leading to the product 2. Other, unexpected, 7-substituted-1,2,3,3a-tetrahydro-3a-methyl-2-phenylimidazo[1,5-a]quinoxalin-4(5*H*)-ones, annulation products, 3a–f, were generated; likely by the addition of two PhNHCH<sub>2</sub>• radicals, to positions 3 and 4 of the quinoxalin-2-ones. The reaction mechanism includes a photoinduced one electron transfer initiation step, propagation steps involving radical intermediates and NPG with radical chain termination steps that lead to the respective products 2a–f and 3a–f and NPG by-products. The proposed mechanism accounts for the strong dependency found for the initial photoconsumption quantum yields on the electron-withdrawing power of the substituent. Therefore, photolysis of common reactants widely used such as NPG and substituted quinoxalin-2-ones may provide a simple synthetic way to the unusual, unreported tetrahydro-imidazoquinoxalinones 3a–f.

### INTRODUCTION

In the last few decades, many studies on the biological properties of quinoxalin-2-one derivatives have been published because of their several pharmacological properties such as: antimicrobial, antifungal, anxiolytic, analgesic, antithrombotic, antitumoral and due to their capacity as inhibitors of the activity of certain enzymes involved in HIV-1 (1–8).

Several works locate the quinoxalin-2-one derivatives inside different proteins receptors, generally close to the ATP-binding pocket. These interactions have been modeled by molecular dynamics docking and in some cases the adduct structures were supported by X-Ray crystallographic studies (9–12). These facts

strongly suggest that the quinoxalin-2-one derivatives might interact with potential electron-donating amino acids residues.

Despite the thoughtful biological, synthetic and pharmacological studies on quinoxalin-2-one derivatives there are relatively few reports on the photochemical and the radical chemistry of these heterocyclic compounds. Some derivatives initiate free radical polymerization by electron transfer from *N*-phenylglycine (NPG) used as an electron donor (13). Photoreduction of quinoxalin-2-ones by amines originates the corresponding dihydroquinoxalin-2-ones or the reductive dimers, depending on the substituent in position 3 of the heterocycle ring (14). Also, efficient [2 + 2] cycloadditions of quinoxalin-2-ones and related oxazinones with alkenes leading to tricyclic azetidines have been reported (14–18).

Ten years ago we studied two 3-phenyl-quinoxalin-2-one derivatives and found a nearly quantitative reversible photoreduction by amines (19). This photoreduction proceeded through a stepwise transference of electron–proton–electron from the amine to the excited triplet of the 3-phenyl-quinoxalin-2-ones, leading to a metastable semireduced anion capable of reverting almost quantitatively to the original quinoxalin-2-ones.

This photoreduction mechanism was further supported by laser flash photolysis experiments which allowed the identification of the photoreduction intermediate absorptions (20). The stepwise electron–proton–electron transfer mechanism observed for quinoxalin-2-one derivatives is similar to the one we reported for the oxoisoaporphines derivatives studied in the last years (21–25). Both kinds of compounds, quinoxalin-2-ones and oxoisoaporphines, contain conjugated C=N and C=O moieties in their structures, which are the groups inducing their photoreactivity toward amines, showing the unusual thermal reversion of metastable semireduced photoproducts.

In this article, we report the result obtained in the photoreduction in acetonitrile by NPG of six 7-substituted-3-methyl-quinoxalin-2(1*H*)-one derivatives, **1a–f**, shown in Chart 1.

We selected NPG as a model reductant amino acid because its radical cation, NPG<sup>•+</sup>, likely present as the carboxylate zwitterion radical PhN(H)<sup>•+</sup>-CH<sub>2</sub>COO<sup>-</sup> has a reported absorption at 460 nm (26), which will be helpful for future laser flash photolysis studies. Together with this absorption, NPG<sup>•+</sup> decarboxylates rapidly (27) at rates >10<sup>8</sup> s<sup>-1</sup>, generating the phenyl-amino-alkyl radical

\*Corresponding author email: jrfonte@ciq.uchile.cl (Julio R. De la Fuente)

<sup>†</sup>This article is part of the Special Issue dedicated to the memory of Elsa Abuin

© 2013 The American Society of Photobiology

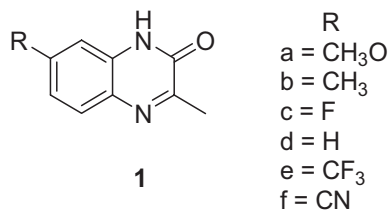


**Chart 1.** Structure of 7-substituted-3-methyl-quinoxalin-2(1H)-one derivatives.

PhNHCH<sub>2</sub>• absorbing at 400 nm (28). The fast decarboxylation of NPG<sup>•+</sup>, Scheme 1, should avoid a back electron transfer to the electron acceptor.

## MATERIALS AND METHODS

**Materials.** Acetonitrile Merck, HPLC grade and acetonitrile-d<sub>3</sub> 99% D, Aldrich, spectroscopic grade were used as received. NPG, Aldrich 97%, was crystallized twice from water before use.

**Synthesis of substituted 3-methyl-2(1H)-quinoxalin-2-ones 1a–f.** Substituted 3-methyl-2(1H)-quinoxalin-2-ones **1a–f** were prepared by the classical reaction of the corresponding *o*-phenyldiamines (1 mmol) by adding drop by drop methyl pyruvate (1.2 mmol) and triethylamine (3 mmol) in ethanol (5,15). Solutions were heated at 80°C for 2 h under nitrogen atmosphere. After 2 h the heating was stopped and the reactants were allowed to cool. The contents of the flask were filtered through celite under reduced pressure and washed with a minimal amount of absolute ethanol. The solvent was removed in vacuum to afford the crude compound, which was purified by flash column chromatography eluted with ethyl acetate:hexane 9:1 and finally crystallized from acetonitrile, to give the pure quinoxalin-2-one derivatives. In reactions where a mixture of isomers in positions 6 and 7 was obtained, the isomers were separated by flash column chromatography using silica gel and THF:1,2-dichloroethane 1:1.

The spectral characterization of **1a–f** by <sup>1</sup>H NMR and HRMS (EI<sup>+</sup>) is in agreement with the expected structures. DMSO-d<sub>6</sub> <sup>1</sup>H and <sup>13</sup>C NMR for the substrates are provided as Supplementary Materials.

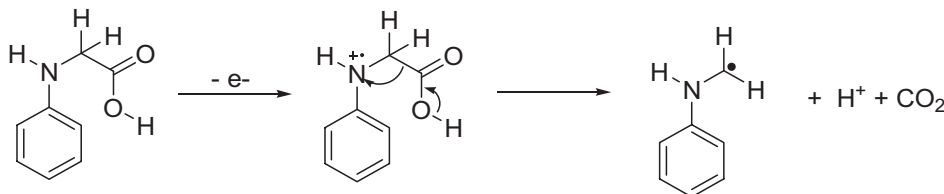
**1a: 7-Methoxy-3-methyl-1H-quinoxalin-2-one**—HRMS (EI<sup>+</sup>) *m/z* calculated for C<sub>10</sub>H<sub>10</sub>N<sub>2</sub>O<sub>2</sub>: 190.07422; found: 190.07420. <sup>1</sup>H NMR (300 MHz, CDCl<sub>3</sub>) δ 11.49 (s, 1H, NH), 7.70 (d, *J* = 8.9 Hz, 1H), 6.92 (dd, *J* = 8.9, 2.6 Hz, 1H), 6.71 (d, *J* = 2.6 Hz, 1H), 3.91 (s, 3H), 2.58 (s, 3H).

**1b: 3,7-Dimethyl-1H-quinoxalin-2-one**—HRMS (EI<sup>+</sup>) *m/z* calculated for C<sub>10</sub>H<sub>10</sub>N<sub>2</sub>O: 174.07932; found: 174.07911. <sup>1</sup>H NMR (300 MHz, CDCl<sub>3</sub>) δ 12.45 (s, 1H, NH), 7.67 (d, *J* = 8.6 Hz, 1H), 7.6 (s, 1H), 7.13 (dd, *J* = 7.6 Hz, 1H), 2.62 (s, 3H), 2.48 (s, 3H).

**1c: 7-Fluoro-3-methyl-1H-quinoxalin-2-one**—HRMS (EI<sup>+</sup>) *m/z* calculated for C<sub>9</sub>H<sub>7</sub>FN<sub>2</sub>O: 178.05424; found: 178.05412. <sup>1</sup>H NMR (300 MHz, CDCl<sub>3</sub>) δ 11.92 (s, 1H, NH), 7.79 (dd, *J* = 8.8, 5.6 Hz, 1H), 7.06 (dd, *J* = 5.5, 2.8 Hz, 1H), 7.03 (t, *J* = 2.7 Hz, 1H), 2.61 (s, 3H).

**1d: 3-Methyl-1H-quinoxalin-2-one**—HRMS (EI<sup>+</sup>) *m/z* calculated for C<sub>9</sub>H<sub>8</sub>N<sub>2</sub>O: 160.06366; found: 160.06344. <sup>1</sup>H NMR (300 MHz, CDCl<sub>3</sub>) δ 11.38 (s, 1H, NH), 7.81 (d, *J* = 8.1 Hz, 1H), 7.49 (t, *J* = 7.1 Hz, 1H), 7.29–7.33 (m, 2H), 2.64 (s, 3H).

**1e: 3-Methyl-7-trifluoromethyl-1H-quinoxalin-2-one**—HRMS (EI<sup>+</sup>) *m/z* calculated for C<sub>10</sub>H<sub>7</sub>F<sub>3</sub>N<sub>2</sub>O: 228.05106; found: 228.05110. <sup>1</sup>H NMR (300 MHz, CDCl<sub>3</sub>) δ 10.31 (s, 1H, NH), 7.92 (d, *J* = 8.4 Hz, 1H), 7.56 (d, *J* = 8.4 Hz, 1H), 7.47 (s, 1H), 2.65 (s, 3H).



**Scheme 1.** Decarboxylation of N-phenylglycine radical cation.

**1f: 7-Cyano-3-methyl-1H-quinoxalin-2-one**—HRMS (EI<sup>+</sup>) *m/z* calculated for C<sub>10</sub>H<sub>7</sub>N<sub>3</sub>O: 185.05891; found: 185.05877. <sup>1</sup>H NMR (300 MHz, CDCl<sub>3</sub>) δ 11.88 (s, 1H, NH), 7.91 (d, *J* = 8.3 Hz, 1H), 7.64 (d, *J* = 1.3 Hz, 1H), 7.59 (dd, *J* = 8.3, 1.6 Hz, 1H), 2.68 (s, 3H).

**HRMS (70 eV) [EI<sup>+</sup>]:** for product **3a**: *m/z* calculated for C<sub>18</sub>H<sub>19</sub>N<sub>3</sub>O<sub>2</sub>: 309.14773; found 309.14766 and for product **3e**: *m/z* calculated for C<sub>18</sub>H<sub>16</sub>F<sub>3</sub>N<sub>3</sub>O, 347.12455; found 347.12462. Poor quality <sup>13</sup>C NMR spectra were obtained due to the low amount of isolated products.

**Steady-state photolysis.** Typically acetonitrile solutions (3 mL) containing 0.1 mM of substrates **1a–f**, with absorbances approximately 1.0 at 366 nm, in the presence of appropriate NPG concentration were saturated with Ar for 20 min, protected from light. Each sample was photolyzed directly in the spectrophotometer with a 150 W low-pressure Hg lamp, equipped with a 366 nm filter in an Agilent 8453 diode array spectrophotometer provided with a stirred cell holder. For the perylene photosensitized reaction, a filter absorbing below 385 nm was used and the photolysis time was limited to 20 min. Stock solutions of each reactant were prepared and mixed in the appropriate proportions before Ar bubbling. During these procedures, the samples were protected from light. Typical concentration in the quartz cell was 0.05 mM perylene, approximately 1 mM NPG and between 0.05 and 0.8 mM, for **1d–f**. The initial concentrations of perylene and NPG were kept constants in these experiments. The photolyzed samples at the higher [**1d–f**] were also analyzed by GC–MS. For these experiments, the photoconsumption was evaluated as the absorbance difference at *t* = 0 and *t* = 20 min:  $Abs_{t=0} - Abs_{t=20 \text{ min}}$ , at each considered wavelength.

**Preparative photolysis.** Preparative photolysis was done in acetonitrile for derivatives **1a** and **e** with solutions containing 150 mg of NPG and approximately 40 mg (1.8–2.1 mmol) of **1e** and **a** respectively, in 150 mL acetonitrile HPLC quality, and bubbled with Ar for 1 h. Photolysis of these solutions, under continuous Ar bubbling and stirring, using a 150 W Black Ray UV lamp equipped with a 366 nm filter, was performed for 2 h. Samples of the products (0.5 mL) were reserved for GC–mass analyses. The remnant was dried out, and seeded in Merck, Silica gel 60F<sub>254</sub> 2 mm thin layer preparative plates, which were eluted with hexane:ethyl acetate 1:1, which showed seven main separated bands. These bands were scraped and extracted in acetonitrile, to prepare samples for GC mass. The fraction of interest was further purified by thin layer chromatography (TLC) with hexane:ethylacetate; 3:1, dried out and dissolved in deuterated acetonitrile for NMR spectroscopy.

**NMR spectroscopy.** <sup>1</sup>H NMR, COSY, HMBC, HMQC and <sup>13</sup>C NMR DEPT 135° were done in a Bruker Advance DRX-400, 400 MHz spectrometer, using tetramethylsilane as the internal standard. Due to the low concentration of the samples, experiments lasted several hours.

**Photoconsumption quantum yields ( $\Phi_{PC}$ ).** Photoconsumption quantum yields ( $\Phi_{PC}$ ) were evaluated from the initial photoconsumption rates,  $V_0$ , measured at the maximum of the lower energy absorption band of the respective substrates **1a–f** and corrected by the initial sample absorption at 366 nm,  $A_{366}$ , against Aberchrome<sup>®</sup> 540 (29), taking  $\Phi_{Aber} = 0.2$  and;  $\epsilon_{Aber}$  at 494 nm as 8200 M<sup>-1</sup> cm<sup>-1</sup>. The expression used was as follows:  $\Phi_{PC} = (V_0/\epsilon_{\lambda_{max}} \times \Phi_{Aber})/[V_{Aber}/\epsilon_{Aber} \times (1 - 10^{-A_{366}})]$ , where  $\epsilon_{\lambda_{max}}$  was the absorption coefficient of **1a–f** at the wavelength maximum and  $V_{Aber}$  the rate of the appearance of absorption at 494 nm. All these experiments were made with 3 mL solutions in acetonitrile at absorbances between 0.9 and 1.1 for [**1a–f**] approximately 0.1 mM and with [NPG] > 1 mM, in the plateau zone.

GC–MS spectral analyses and HRMS were obtained using a MAT 95 XP Thermo Finnigan Spectrometer at 70 eV EI<sup>+</sup>. High-resolution mass spectra were made at 70 eV (Positive) with reference perfluoro kerosene. Low-pressure CI analyses, using methanol as reagent, were done in a Varian 421-GC with a 220-MS detector. Mass–mass tandem spectra were obtained in a Thermo Scientific Quantum XLS triple quadrupole detector, in a Trace GC,

with a column Restek Rtx-5MS 30 m  $\times$  0.25 mm  $\times$  0.25  $\mu$ m GC-MS/MS. Oven method: Initial temperature 70°C, initial time 2.0 min, ramp 1°C/min, final temperature 300°C, hold time 4.0 min and constant flow of 1 mL/min; carrier gas He.

Laser flash photolysis experiments were performed on the modernized instrument described previously (20,23,25). Now it was provided with a Continuum Surelite I 10 Hz Q-switched Nd-YAG laser and the signals were now captured by a WaveSurfer 600 MHz LeCroy oscilloscope. Software written in National Instrument LabViews 8.0 controls the laser, monochromator and shutters and captured the data which are fed to Igor Pro 6.3 written program for treatment and display. The system is provided with a peristaltic pump and a 0.5 mL flow cell to assure the continuous renovation of solutions. Optimal results were obtained with solutions with absorbances between 0.4 and 0.6 at the 355 nm excitation wavelength. The laser power impinging the cell was attenuated using glass plates to  $\sim$ 10 mJ per pulse. Quenching experiments were typically made with solutions (3 mL) of substrates bubbled with Ar for 20 min in 10 mm square quartz cells sealed with a septum. After purging, aliquots of quenchers were added and the lifetimes  $\tau$  at definite wavelengths measured. Quenching constants were obtained from slopes of Stern-Volmer-type plots of  $1/\tau$  vs [quencher] which resulted in linear regression with  $r > 0.95$  in all of the experiments.

Transient spectra in the presence of 1,4-diazabicyclo[2.2.2]octane (DABCO) or NPG were obtained with Ar bubbled 250 mL acetonitrile solutions containing 0.1 mM of the quinoxalin-2-one. These solutions were monitored in the 0.5 mL flow cell at a flow rate of 1 mL/min taking a mean of five laser shots for each monitored wavelengths at each DABCO or NPG concentration used. The Ar bubbling was maintained during the whole experiment.

## RESULTS AND DISCUSSION

### Steady-state photolysis

All of the quinoxalin-2-one derivatives studied were photostable in air-saturated acetonitrile solutions, irrespective of the presence of NPG. In argon-saturated solutions, a fast photoreaction with significant spectral changes occurred. One or several isosbestic points appeared, depending on the quinoxalin-2-one substituent. These isosbestic points strongly suggest the formation of a single product or a mixture in a constant molar ratio. The absence of photoreaction in air-saturated solutions strongly points to a reac-

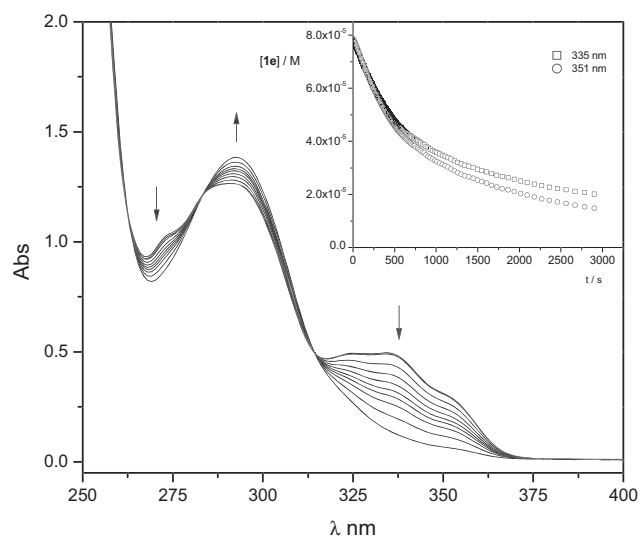


**Figure 1.** Photolysis of 0.1 mM  $\text{CF}_3$ -substituted derivative **1e** in the presence of 1.0 mM *N*-phenylglycine. The arrows show the absorbance changes. The inset shows the kinetic traces at 335 nm ( $\square$ ) and 351 nm ( $\circ$ ) used to evaluate the initial rates for photoconsumption quantum yields.

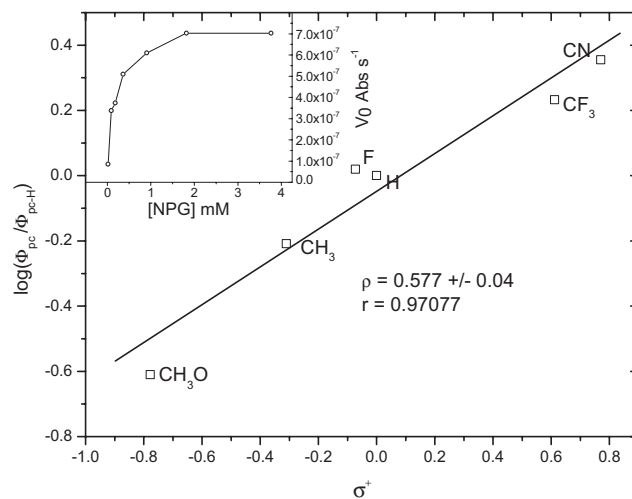


**Figure 2.** Hammett plot for the  $\Phi_{\text{pc}}/\Phi_{\text{pc-H}}$  vs the electrophilic substituent parameter  $\sigma^+$  often used for radical reactions. The inset shows the [*N*-phenylglycine] effect in the initial photoconsumption rate,  $V_0$ , for 0.1 mM 7-F-derivative **1c**,  $V_0$  expressed  $\text{Abs s}^{-1}$ .

**Table 1.** Photoconsumption quantum yields for the photoreduction of 7-substituted-3-methyl-quinoxalin-2-ones by *N*-phenylglycine with the respective electrophilic substituent Hammett parameter  $\sigma^+$ .

Derivative Substituent	1a $\text{CH}_3\text{O}$	1b $\text{CH}_3$	1c F	1d H	1e $\text{CF}_3$	1f CN
$\sigma^+$	-0.778	-0.311	-0.073	0.0	0.612	0.659
$\Phi_{\text{pc}}^*$	0.27	0.68	1.15	1.10	1.88	2.49

\*Photoconsumption quantum yields are the average of two or more measures and have a bounded 5% error.

tion from the quinoxalin-2-ones triplet manifold. As an example of these photoreactions, Fig. 1 is included, showing the 7- $\text{CF}_3$ -derivative **1e** photoreduction by NPG with three isosbestic points in the spectral region of interest.

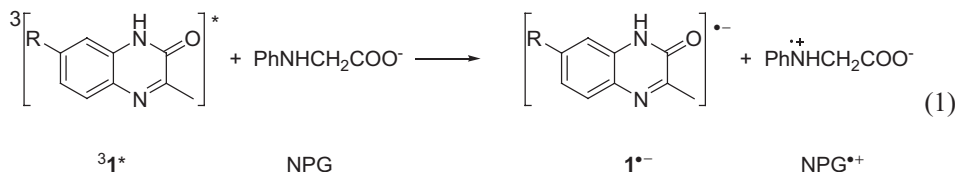
For all of the derivatives studied, the initial photoconsumption rates were strongly dependent on the NPG concentration, increasing monotonically up to plateau values at  $[\text{NPG}] \geq 1.5$  mM, for  $\sim$ 0.1 mM quinoxalin-2-ones, (for the 7-fluor derivative, **1c**, see inset in Fig. 2). By measuring initial rates, at  $[\text{NPG}]$  in the plateau region, photoconsumption quantum yields,  $\Phi_{\text{pc}}$ , were evaluated as described in the Experimental Section. The values determined for  $\Phi_{\text{pc}}$  were as low as 0.27 for the 7- $\text{CH}_3\text{O}$  derivative, **1a**, to a surprisingly high 2.49 for the 7-CN derivative, **1f**. This large  $\Phi_{\text{pc}}$  value cannot be explained by considering only a photochemical reaction between electronically excited **1** and NPG, suggesting a radical chain reaction between photochemically NPG-generated radicals and likely, the ground state quinoxalin-2-one.

Interestingly, the  $\Phi_{\text{pc}}$  increased with an increase in the electron-withdrawing power of the substituent (Table 1) and correlated well with the Hammett electrophilic substituent  $\sigma^+$  parameter (30), with a  $\rho = 0.577 \pm 0.04$  ( $r = 0.9708$ ), as shown in Fig. 2. The observed correlation strongly suggests that the reaction mechanism is the same for all the derivatives studied, irrespective of the quinoxalin-2-one substituent.

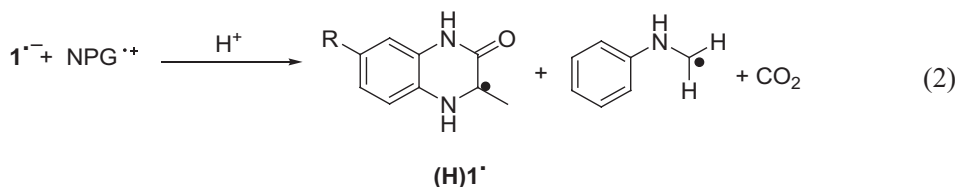
Positive  $\rho$  values, similar to those obtained in this work, have been related to radical addition reactions of alkyl radicals to the aromatic nuclei of substituted toluenes (31), to aminoxyl radical addition to arylketenes (32), to the ratio between addition and

electron abstraction on aromatic rings (33–35) and to the addition of thiyl radicals to vinyl monomers (36,37).

Taking into account the stepwise photoreduction reported for 3-phenyl-quinoxalin-2-ones (19,20), the lack of any photoreaction for **1a–f** derivatives in aerated samples, and some laser flash photolysis results (*vide infra*) that showed that the first step of photoreaction is mainly a one electron transfer from the NPG, as  $\text{PhNHCH}_2\text{COO}^-$ , to the excited triplet state of the substituted 3-methyl-quinoxalin-2-one, **31**, it can be proposed that the formation of a ion radical pair, Eq. (1) is the first step of the photoreaction.

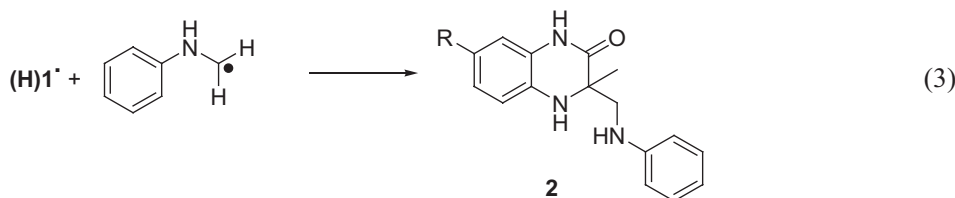


Reaction of  $\mathbf{1}^{\bullet-}$  with media  $\text{H}^+$  from the NPG should lead to the captodative-stabilized radical  $(\text{H})\mathbf{1}^{\bullet}$  and by decarboxylation of  $\text{NPG}^{\bullet+}$  should be formed the radical  $\text{PhNHCH}_2^{\bullet}$ , Eq. (2). The quinoxalin-2-one radical anion  $\mathbf{1}^{\bullet-}$  is similar to those reported previously as intermediaries by us for the amine photoreduction of 3-phenyl-quinoxalin-2-ones (19,20).



On the other hand, by considering a competitive hydrogen transfer from the NPG to the excited quinoxalin-2-one, a fast formation of  $(\text{H})\mathbf{1}^{\bullet}$  and the  $\alpha$ -aminoalkyl radical  $\text{PhNH}\dot{\text{C}}\text{HCOO}^-$  which after protonation also decarboxylate (27,28), leading to the same radicals shown in Eq. (2) can be expected. Flash photolysis experiments (*vide infra*) show evidence of this competitive contributing reaction path.

The combination of the two radicals  $\text{PhNHCH}_2^{\bullet}$  and  $(\text{H})\mathbf{1}^{\bullet}$  should lead to product **2**, Eq. (3), with a nominal mass  $M + 107$ , where  $M$  is the molecular mass of the original 7-substituted-3-methyl-quinoxalin-2-one.



### Product GC-MS analysis

Electronic impact, EI GC-mass analysis of the photolyzed samples, reveals several NPG oxidation products such as: aniline ( $\text{PhNH}_2$ ,  $m/z = 93$ ) and *N,N'*-diphenylethylenediamine ( $(\text{PhNHCH}_2)_2$ ,  $m/z = 212$ ), which are confirmed by comparison with the respective standards, and *N*-methylenebenzenamine ( $\text{PhN}=\text{CH}_2$ ,  $m/z = 105$ ), which was identified by its database NIST© mass spectra. In addition, NPG excess with  $m/z = 151$  and the remnant quinoxalin-2-ones with their respective  $m/z = M$ , for each derivative **1a–f** were also detected.

The presence of *N*-methylenebenzenamine and *N,N'*-diphenylethylenediamine in the product mixtures strongly supports the involvement of  $\text{PhNHCH}_2^{\bullet}$  in the photoreaction and hence the decarboxylation reaction of Scheme 1. Among the mentioned NPG products, other unidentified NPG products with  $m/z$ : 223,

230 and 340 appeared in all of the experiments, independent of the quinoxalin-2-one substituent.

For all of these experiments, the EI GC-mass analysis showed only two quinoxalin-2-one main products for each of the **1a–f** products investigated. These products can be easily recognized because their  $m/z$  ratios differ in the substituent masses. The first product, appearing at lower retention times, had a  $m/z = M + 2$ , and the second, totally unexpected products, named **3**, appearing at longer retention times, had a  $m/z = M + 119$ , where  $M$  is the nominal mass of the respective 7-substituted-quinoxalin-2-one derivatives **1a–f**.

In these analyses, the expected product **2**, from the radical addition, Eq. (3), with  $m/z = M + 107$  was not found. The detection of a product with  $m/z = M + 2$  suggests the formation of the dihydro-quinoxalin-2-one derivatives by the reduction in the imino moiety. To confirm the  $m/z$  ratio for these products, a more mild chemical ionization detection (CI GC-MS) was used for the analyses of photolyzed mixtures for substrates **1a** and **e**. We selected these derivatives because their substituents have similar but opposed  $\sigma^+$  values. The results of these analyses show products **2a** and **e** appearing with  $m/z = M + 108$ , with  $M$  being the mass of **1a** or **e**. These findings agree with the addition of  $\text{PhNHCH}_2\cdot$  plus the extra proton added by the CI. Therefore, by extension, the expected products **2a-f**, are actually formed with  $m/z = M + 107$  molecular ion, which cannot be detected by EI. Under the same conditions, that is CI GC-MS, the second quinoxalin-2-one products **3a** and **e**, appeared with  $m/z = M + 120$ , confirming that the molecular ion  $m/z$  corresponded to those obtained by EI mass analyses. Again  $M$  is the mass of products **1a-f**. These results are summarized in Table 2.

These results clearly show that the expected addition products **2a-f** are present after the photolysis and that the molecular ion of product **3** has  $m/z = M + 119$ , suggesting the involvement of at least two  $\text{PhNHCH}_2\cdot$  in their formation. Moreover, for both products **2** and **3**, the  $m/z$  ratios are odd for all the substituents with the exception of CN. Therefore, according to the nitrogen rule, these molecular ion masses confirm an odd number of  $N$  atoms in both kinds of products, with the exception of the CN-substituted product **3f**.

### Mass spectra analysis

Mass spectra of products **2a-f** obtained by CI show similar features for the substrates studied, with the release of two main neutral fragments; one with nominal mass 93, which is independent of quinoxalin-2-one substituent, and another dependent on it, with mass  $M + 2$ , where  $M$  is the quinoxalin-2-one mass. This fragment can explain the  $m/z$  ratio observed when using electronic impact ionization. The loss of 93 mass units, likely aniline, accounts for the observed peaks at  $m/z = 205$  and  $243$ , shown in Fig. 3, for the products **2a** and **e**, respectively. The peak at  $m/z = 106$ , likely  $\text{Ph}^+\text{NH}=\text{CH}_2$ , accounts for the loss of the  $M + 2$  neutral fragments. These ionized fragments probably are those observed in EI mass spectra. The fragmentation pattern, the same for all of the substrates studied, fits well the proposed structure for products **2a-f**.

In the same manner as for the products **2a-f**, a regular fragmentation pattern was found for the products **3a-f**, in the EI GC-mass experiments. For all the photolyzed substrates, together with the molecular ion with  $m/z = M + 119$ , the mass spectra

**Table 2.** Nominal  $m/z$  ratio for the products molecular ions generated in the photoreduction by *N*-phenylglycine of 7-substituted-3-methyl-quinoxalin-2-ones **1a-f**.

Derivative	1a	1b	1c	1d	1e	1f
Substituent	$\text{CH}_3\text{O}$	$\text{CH}_3$	F	H	$\text{CF}_3$	CN
Substituent mass	31	15	19	1	69	26
$m/z$ product <b>2</b>	297	281	285	267	335	292
$m/z$ product <b>3</b>	309	293	297	279	347	304

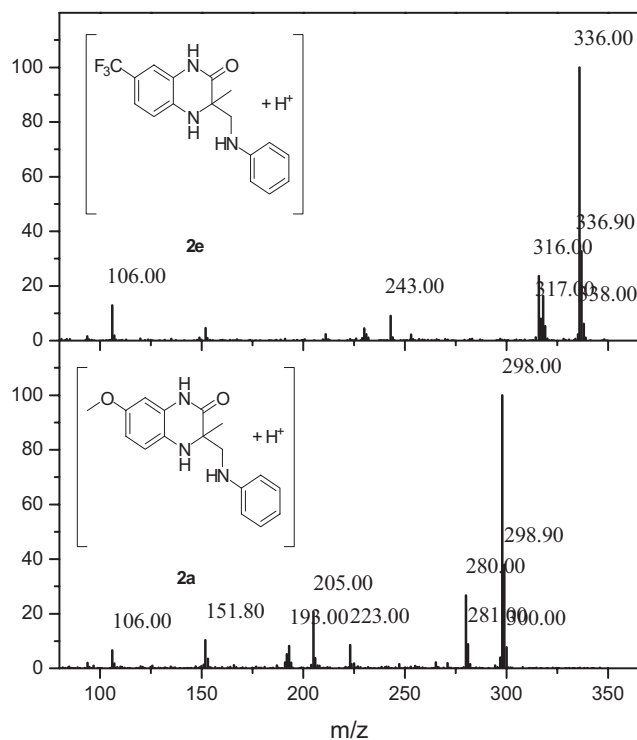


**Figure 3.** Mass spectra for the molecular ions obtained by chemical ionization for: the  $\text{CF}_3$ -derivative product **2e** and for the  $\text{CH}_3\text{O}$ -derivative product **2a**. For the molecular ions, the  $m/z$  ratio corresponds to  $M + 1$ ,  $M$  being the molecular mass of products **2a-e**.

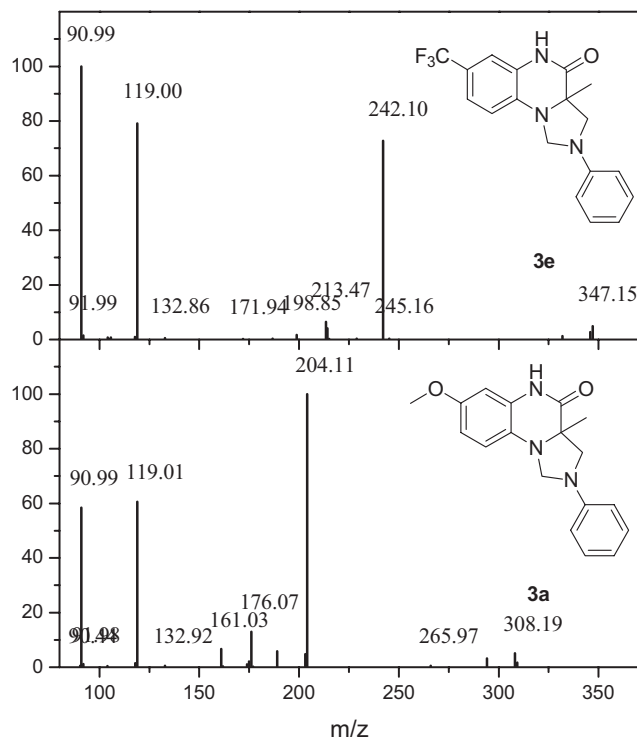
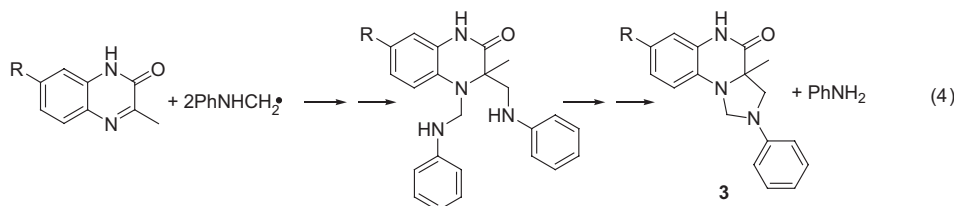


**Figure 4.** Mass-mass spectra for product **3** molecular ions show the common fragments with  $m/z = 91$  and  $119$  and those corresponding to  $M + 14$  fragments; for the  $\text{CF}_3$ -derivative **3e**,  $m/z = 242$ ; and B) for the  $\text{CH}_3\text{O}$ -derivative **3a**,  $m/z = 204$ .

show two fragments with  $m/z$  91 and 119 irrespective of the substrate **1a–f**. Others fragments derived from the loss of 105 mass units with respect to the molecular ions, with  $m/z = M + 14$  were found for all the derivatives. In Fig. 4 are shown the tandem mass–mass spectra corresponding to the molecular ions **3a** and **e**, showing clearly the common 91 and 119 fragments, and those with  $m/z$  204 and 242 observed for **3a** and **e**, respectively. According to the nitrogen rule, these last fragments have an even number of N atoms in their structure. Thus, these fragments with



$m/z = M + 14$  suggest a  $\text{CH}_2$  bounded to the original quinoxalin-2-ones **1a–f** and one N atom less than products **3a–f**.

### Product isolation and NMR analysis

The preceding mass spectra results do not give enough information to elucidate the structure of the products. Therefore, we did some preparative photolysis with **1a** and **e**, and the products were separated using TLC. The details are given in the Experimental Section. Each fraction was extracted and analyzed by GC mass searching for products **2** and **3**. In these fractions, the same above-mentioned NPG oxidation products were found. One of these fractions contained nearly pure product **3**. But product **2** was not found in any of the fractions, likely due to its decomposition by a reaction with the TLC silica.

The fraction containing **3a** or **e** was further purified by TLC, dried out and dissolved in  $\text{CD}_3\text{CN}$  for  $^1\text{H}$  NMR, COSY, HMBC, HMQC and  $^{13}\text{C}$  NMR DEPT 135° experiments, which were employed to elucidate their structure. The NMR results are summarized in Table 3 and the  $^1\text{H}$  NMR spectrum for **3e** is shown in Fig. 5.

By extending these results to the other derivatives, which show the same EI mass spectral pattern, products **3a–f** can be unequivocally identified as the respective 7-substituted-1,2,3,3a-tetrahydro-3a-methyl-2-phenylimidazo[1,5-a]quinoxalin-4(5H)-ones. Moreover, high-resolution mass spectra, HRMS, were determined for **3a** and **f**, with expected masses 309.14773 and 347.12455 and molecular ions were found with  $m/z$  309.14766 and 347.12462, respectively. These values differ from the calculated exact mass by less than 0.25 ppm, confirming the proposed structures. By considering these structures it is possible to account for the fragments observed in mass spectra as shown in Scheme 2.

To rule out other possible sources of product **3**, we tested the photoreactions of **1a** and **e** with *N,N'*-diphenylethylenediamine ( $\text{PhNHCH}_2$ )<sub>2</sub> and aniline, which appeared as NPG oxidation products. All of these attempts were unsuccessful rejecting any reaction with these NPG products.

The present results provide strong evidence that product **3** formation should involve the attack of two  $\text{PhNHCH}_2\cdot$  radicals derived from the NPG, followed by the elimination of aniline, as

shown in Eq. (4). This aniline elimination may occur by protonation of one of the  $\text{PhNHCH}_2$  tethered to the quinoxalin-2-one followed by the nucleophilic displacement of aniline. However, this reaction requires two  $\text{PhNHCH}_2\cdot$  radicals, which have to be generated in a radical chain reaction to explain the photoconsumption quantum yields observed for the most electron-withdrawing substituted derivatives **1e** and **f**, see Table 1 and Fig. 2.

To generate the two  $\text{PhNHCH}_2\cdot$  radicals needed to obtain product **3**, two electron or hydrogen transfers steps from NPG to

**1**, Eq. (1), followed by decarboxylation of the NPG radical cations or their  $\alpha$ -aminoalkyl radical are required. Hence, the limit for the quinoxalin-2-one photoconsumption quantum yield,  $\Phi_{\text{pc}}$ , leading only to product **3** cannot be larger than 0.5. On the other hand, by assuming that the reaction leads only to product **2**, a  $\Phi_{\text{pc}} = 1$  can be expected. Any combination of both products **2** and **3** should give  $\Phi_{\text{pc}}$  values below 1.0 but, for **1c–f**, values are larger than 1.0 and for **1e** and **f** the observed values are 1.88 and 2.49, respectively. Therefore, a purely photochemical reaction cannot explain the experimental results, suggesting a chain radical propagation, leading to  $\text{PhNHCH}_2\cdot$  radicals. If this assumption is true, generating the  $\text{PhNHCH}_2\cdot$  radicals in the presence of the quinoxalin-2-ones, but without involving any of their excited states, the same photoproducts **2** and **3** should be found.

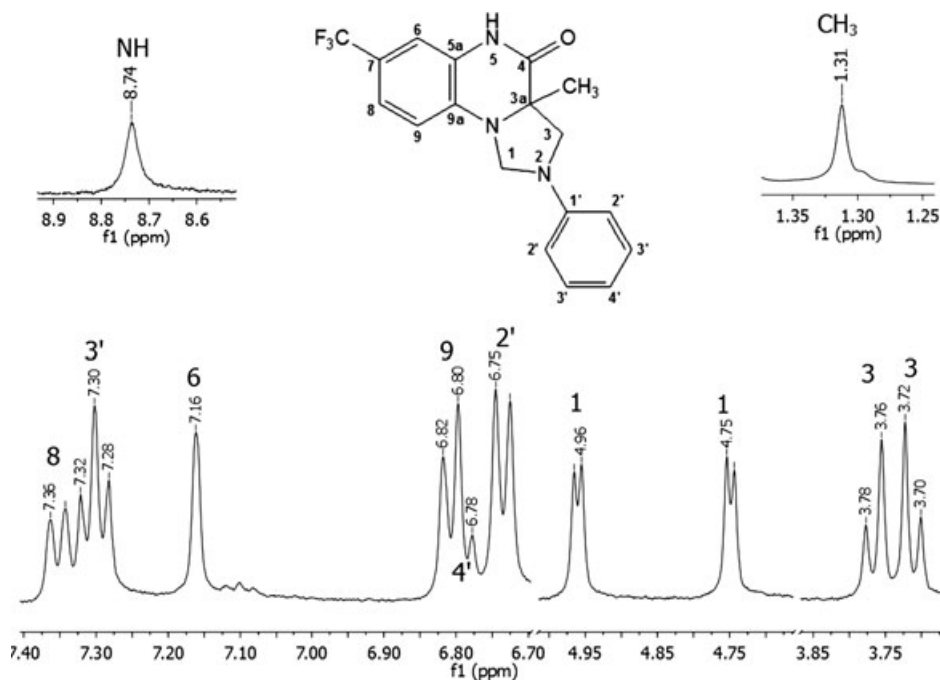
### Sensitized photolysis

It was reported that the photolysis of NPG sensitized by polycyclic aromatic hydrocarbons, among the perylene, leads to the  $\text{PhNHCH}_2\cdot$  radicals by electro-proton transfer (38). Perylene which absorbs at longer wavelengths to not excite simultaneously some of the substrates, **1d–f**, seems a good sensitizer. Thus, using the proper cut-off filter that transmits for  $\lambda > 385$  nm, we can selectively excite perylene in the presence of substrates **1d–f** and NPG. In these experiments, the perylene and NPG concentration were kept constant, while changing the substrate **1d–f** concentrations. The use of perylene as a photosensitizer precluded energy transfer to the quinoxalin-2-ones, thus any reaction which can be observed should be attributed to the  $\text{PhNHCH}_2\cdot$  radicals formed by proton transfer from NPG to excited perylene (38,39). Details about this photosensitized reaction are given in the Experimental Section. As we expected in the GC-mass analyses of these samples, we found the respective products **2d–f** and **3d–f**, confirming the radical character of the reaction. Moreover, by increasing the quinoxalin-2-one concentration at constant [perylene] and [NPG], an increase in the consumption of NPG and **1d–f**, was observed, and concomitantly perylene consumption decreased, as shown in Fig. 6 for **1d**. These results show that consumption increased by a factor of ~3 and 5 for **1d** and NPG, respectively, for a 7.5-fold increase in product **1d**, at the same photon flux. Similar results were obtained with the other

**Table 3.**  $^1\text{H}$  and  $^{13}\text{C}$  chemical shifts  $\delta$  [H-X, multiplicity,  $J(\text{H,H})$  (Hz)]\* of 3a-Methyl-2-phenyl-7-trifluoromethyl-1,2,3,3a-tetrahydro-5H-imidazo[1,5-a]quinoxalin-4-one, **3e**, and 7-methoxy-3a-methyl-2-phenyl-1,2,3,3a-tetrahydro-5H-imidazo[1,5-a]quinoxalin-4-one, **3a**.

Position	<b>3e</b>			<b>3a</b>		
	$\delta(^1\text{H})$	$\delta(^{13}\text{C})$	HMBC <sup>†</sup>	$\delta(^1\text{H})$	$\delta(^{13}\text{C})$	HMBC <sup>†</sup>
1c	4.75 [H-1, d, $J(1, 1) = 4.0$ ] <sup>‡</sup> 4.97 [H-1, d, $J(1, 1) = 4.0$ ] <sup>‡</sup>	62.9 <sup>¶</sup>	3, 3a	4.71 [H-1, d, $J(1, 1) = 3.0$ ] <sup>‡</sup> 4.83 [H-1, d, $J(1, 1) = 3.0$ ] <sup>‡</sup>	63.3 <sup>¶</sup>	3, 3a
3c	3.71 [H-3, d, $J(3, 3) = 8.7$ ] <sup>‡</sup> 3.77 [H-3, d, $J(3, 3) = 8.7$ ] <sup>‡</sup>	53.9 <sup>¶</sup>	CH <sub>3</sub> , 3a, 4	3.64 [H-3, d, $J(3, 3) = 8.5$ ] <sup>‡</sup> 3.76 [H-3, d, $J(3, 3) = 8.5$ ] <sup>‡</sup>	54.2 <sup>¶</sup>	CH <sub>3</sub> , 3a, 4
3a	—	62.1	—	—	62.0	—
4(C=O)	—	167.0	—	—	167.0	—
5	8.74 [N-H, s] <sup>§</sup>	—	—	8.3 [N-H, s]	—	—
5a	—	126.6	—	—	120.6	—
6	7.16 [H-6, s]	111.8	5a, 7, 8	6.34 [H-6, s]	99.7	5a, 7, 8
7	—	133.7	—	—	156.7	—
8	7.35 [H-8, d, $J(8, 9) = 8.3$ ]	121.2	6, 7, 9, 9a	6.42 [H-8, d, $J(8, 9) = 8.6$ ]	103.3	6, 7, 9, 9a
9	6.81 [H-9, d, $J(9, 8) = 8.3$ ]	112.4	5a, 7, 8, 9a	6.83 [H-9, d, $J(9, 8) = 8.6$ ]	116.3	5a, 7, 8, 9a
9a	—	126.7	—	—	120.9	—
1'	—	146.1	—	—	146.0	—
2'	6.74 [H-2', d, $J(2', 3') = 7.9$ ]	112.3	1', 3', 4'	6.72 [H-2', d, $J(2', 3') = 8.0$ ]	111.7	1', 3', 4'
3'	7.30 [H-3', t, $J(3', 2', 4') = 7.9$ ]	129.0	1', 2', 4'	7.29 [H-3', t, $J(3', 2', 4') = 7.6$ ]	129.1	1', 2', 4'
4'	6.80 [H-4', t] <sup>  </sup>	117.5	2', 3'	6.77 [H-4', t, $J(4', 3') = 7.3$ ]	116.8	2', 3'
CH <sub>3</sub>	1.31[s]	18.3	3, 3a, 4	1.23	16.9	3, 3a, 4
OCH <sub>3</sub>	—	—	—	3.80	54.8	7

\*In ppm from TMS. <sup>†</sup> $^{13}\text{C}$ ,  $^1\text{H}$  HMBC connectivity. <sup>‡</sup>H-1 and H-3 are diastereotopic protons. <sup>§</sup>N-H signal disappeared when D<sub>2</sub>O was added. <sup>||</sup>The H-4' triplet signal is overlapped by the H-9 doublet signal. The integration 2 corresponds to this couple of signals. <sup>¶</sup>Negative phase in  $^{13}\text{C}$  NMR DEPT 135° spectrum.

**Figure 5.** Signal assignment for  $^1\text{H}$  NMR spectrum in  $\text{CD}_3\text{CN}$  for product **3e**. Atom numbering is that shown in the structure and in Table 3. There is a signal at 8.74 ppm, corresponding to NH at position 5, which disappears by adding D<sub>2</sub>O.

derivatives studied, supporting a radical chain reaction generating  $\text{PhNHCH}_2\cdot$  radicals, hence explaining the larger  $\Phi_{\text{pc}}$  for **1e-f**.

#### Laser flash photolysis

All these quinoxalin-2-ones **1a-f** show strong transient absorptions between 350 and 450 nm that were quenched by NPG and DABCO with rate constants close to diffusion limit ( $1.2$  to  $7.5 \times 10^9 \text{ M}^{-1} \text{ s}^{-1}$ ) for NPG and one or two magnitude order

lower for DABCO ( $8.1 \times 10^7$  to  $9.2 \times 10^8 \text{ M}^{-1} \text{ s}^{-1}$ ). These quenching constants do not show dependency on the substituent's nature. The obtained values are in line with the reported oxidation potential of 0.99 and 0.60 V vs SCE for NPG (**38**) and DABCO (**40**), respectively. Therefore, the quenching processes should be mainly attributed to a one electron transfer from the NPG or DABCO to the **1a-f** excited triplet state with the generation of the corresponding radical ion pair. Figure 7 shows the triplet-triplet transient absorption spectra obtained for derivative

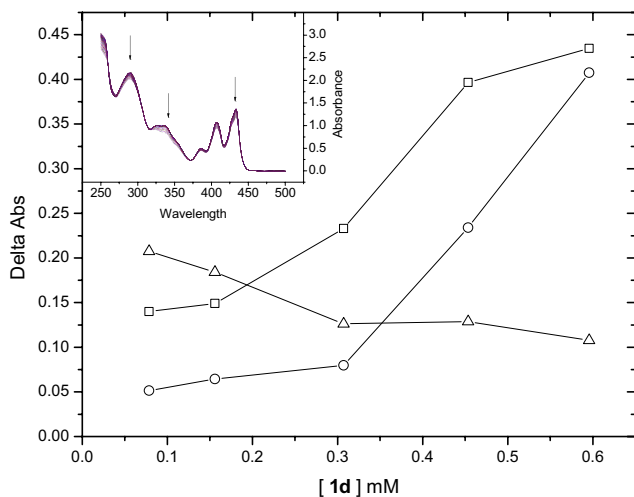
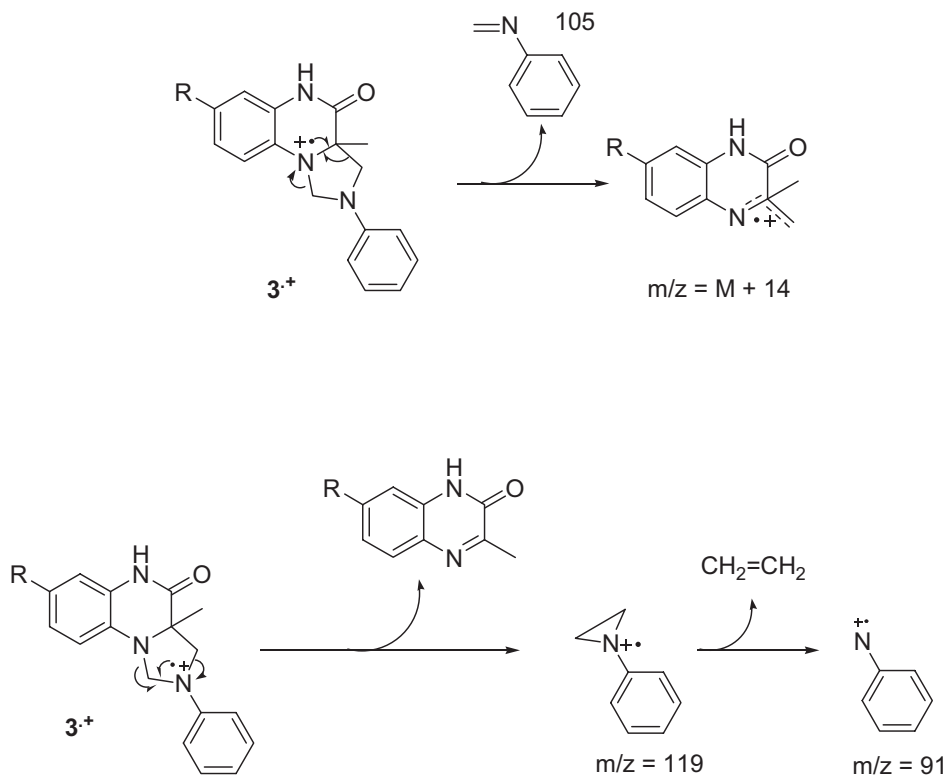


**Figure 6.** Photoconsumption evaluated as  $(Abs_{t=0} - Abs_{t=20 \text{ min}})$  at 336 nm ( $\square$ ), 290 nm ( $\circ$ ) and 433 nm ( $\Delta$ ), corresponding to the nonsubstituted 3-methyl-quinoxalin-2-one **1d**, *N*-phenylglycine (NPG) and perylene, respectively. The inset shows absorbance changes in the sensitized photoreaction of 0.05 mM perylene, 0.9 mM NPG and 0.3 mM **1d**. The arrows show the direction of the absorbance changes.

**1d** in acetonitrile with a maximum at 400 nm, and the spectra obtained in the presence of DABCO at delays of 0.5 and 15  $\mu\text{s}$  after the laser pulse with absorption maxima at 430 and 380 nm, respectively. The spectra obtained in the presence of DABCO were attributed to the radical anion **1d**<sup>•-</sup> at 0.5  $\mu\text{s}$  and to the (**H**)**1d**<sup>•</sup> generated by proton transfer from adventitious water to **1d**<sup>•-</sup> after a 15  $\mu\text{s}$  delay. The (**H**)**1d**<sup>•</sup> absorption band at 380 nm increases when water is added to the acetonitrile confirming our assignment, the  $[\text{H}_2\text{O}]$  effect on  $\Delta\text{OD}$  at 380 nm is shown in the

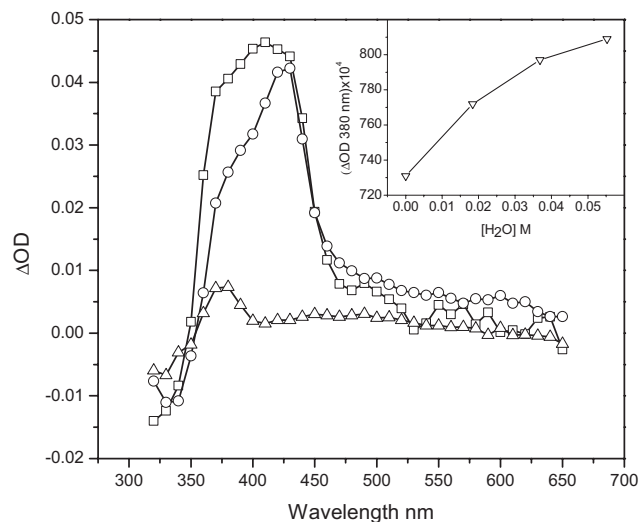


**Figure 7.** Time-resolved absorption spectra for **1d** excited state triplet ( $\square$ ) 1.0  $\mu\text{s}$  after the laser pulse with  $\lambda_{\text{max}} = 410 \text{ nm}$ ; the anion radical **1d**<sup>•-</sup> at  $\lambda_{\text{max}} = 430 \text{ nm}$  ( $\circ$ ) generated in the presence of 1 mM DABCO 0.5  $\mu\text{s}$  after the laser pulse; and the hydrogenated radical (**H**)**1d**<sup>•</sup> at  $\lambda_{\text{max}} = 380 \text{ nm}$  ( $\Delta$ ) after 15  $\mu\text{s}$  delay. The inset shows the effect of  $[\text{H}_2\text{O}]$  on the maximal absorption of (**H**)**1d**<sup>•</sup> at  $\lambda_{\text{max}} = 380 \text{ nm}$ .

inset of Fig. 7. Similar behavior was observed for the other derivatives and can be represented by Eq. (5).



In the presence of NPG, a more complex behavior was observed, see Fig. 8; shortly after the laser shot, the transient

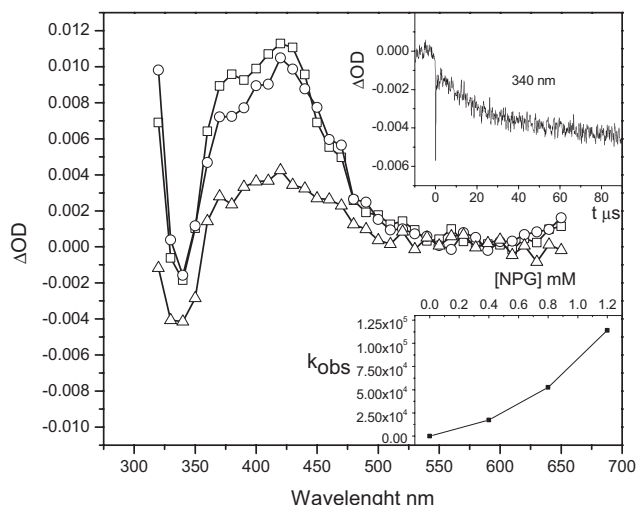
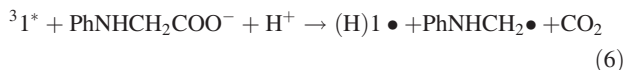


**Figure 8.** Transient spectra for 0.7 mM **1d** in the presence of 1 mM NPG at delays of: 0.5, 5 and 80  $\mu\text{s}$ , ( $\square$ ), ( $\circ$ ) and ( $\Delta$ ), respectively. The upper inset shows the ground depletion at 340 nm and the lower inset shows the effect of [*N*-phenylglycine] on the ground depletion pseudo first-order rate constant decay  $k_{\text{obs}}$ .

spectrum shows a maximum at 430 nm, a secondary maximum at 380 nm and a shoulder at 460 nm. During the first 5  $\mu\text{s}$ , the absorption at 460 nm increases showing the presence of at least three species, while the kinetic traces at 430 and 380 nm evolve differently. More interesting is the strong ground depletion observed at 340 nm (upper inset in Fig. 8) that can be interpreted as showing the consumption of the ground state **1d**. Moreover, the decay rate of this ground depletion depends strongly on the NPG concentration increasing with the [NPG] as shown in the lower inset of Fig. 8. This plot was obtained by adjusting pseudo first-order kinetics to the depletion.

To gain more insight for the spectral assignment, we compared the spectra obtained at short time after the laser pulse in the presence of DABCO and NPG subtracting the spectrum attributed to **1d**<sup>-</sup> to the normalized spectrum obtained in presence of NPG. This difference spectrum, shown in Fig. 9, shows a clear absorption between 440 and 480 nm which can be attributed to NPG<sup>•+</sup> as was reported for the NPG radical cation in water (26). With this absorption also appears a band with maximum at 360 nm which, based on the results in the presence of DABCO and [H<sub>2</sub>O] effect, we assigned to the hydrogenated radical (H)**1d**<sup>•</sup>. This absorption appears shortly after the laser pulse suggesting an early contribution of hydrogen transfer from the NPG to the excited quinoxalin-2-one. This process, Eq. (6), should lead to the hydrogenated radical (H)**1d**<sup>•</sup> and PhNH<sup>•</sup>CHCOO<sup>-</sup> that after decarboxylation should lead to PhNHCH<sub>2</sub><sup>•</sup> (27,28).



In the difference spectrum, another strong absorption with a maximum below 320 nm (below our experimental detection limits) and a shoulder centered at 400 nm were observed and may be tentatively identified with those reported for PhNHCH<sub>2</sub><sup>•</sup> (28), which are probably overlapped with the absorptions of other transient species. Among the aforementioned species it is possi-

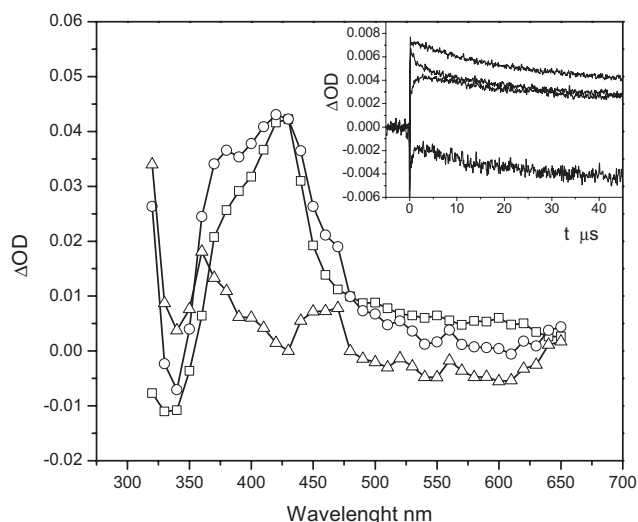


**Figure 9.** Radical anion **1d**<sup>-</sup> ( $\square$ ) spectrum obtained in the presence of DABCO; normalized spectrum of **1d** in the presence of 1 mM *N*-phenylglycine (NPG) ( $\circ$ ) and the resulting spectrum after subtraction of **1d**<sup>-</sup> ( $\Delta$ ); ( $\Delta = \circ - \square$ ) showing the absorption of NPG<sup>•+</sup> between 440 and 480 nm; a maximum at 360 nm attributed to (H)**1d**<sup>•</sup> and a shoulder at 410 nm and a not resolved absorption band with maximum below 320 nm attributed to PhNHCH<sub>2</sub><sup>•</sup>. The inset shows the kinetics profiles of **1d** in the presence of 1 mM NPG; from up to down at 430, 380, 460 and 340 nm, respectively.

ble to consider the presence of PhN<sup>-</sup>CH<sub>2</sub>COO<sup>-</sup> generated by deprotonation of the NPG<sup>•+</sup> ( $\text{p}K_a = 7.35$ ) (26). This radical has similar absorption bands to those reported for PhNHCH<sub>2</sub><sup>•</sup> (28) and cannot be totally ruled out. However, although this radical centered in N may be present, it cannot explain the formation of products **2** and **3**. Therefore, shortly after the pulse the absorption spectra in the presence of NPG should be mainly attributed to the contributions of: **1d**<sup>-</sup>; NPG<sup>•+</sup>; (H)**1d**<sup>•</sup>; PhNHCH<sub>2</sub><sup>•</sup> and likely other unidentified species. It is worthy to note that the absorption contributions that we attributed to: **1d**<sup>-</sup>; NPG<sup>•+</sup> and (H)**1d**<sup>•</sup> are still evident in the spectrum 80  $\mu\text{s}$  after the laser pulse as can be seen in Fig. 8.

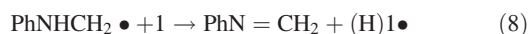
The inset in Fig. 9 shows the decays at the wavelengths of the different maxima and shoulders observed for the transient in the presence of NPG. While in the first 5  $\mu\text{s}$  it can be seen a secondary growth of the absorption attributed to NPG<sup>•+</sup> at 460 nm occurring simultaneously with the decay of (H)**1d**<sup>•</sup> at 380 nm, suggesting that the formation of NPG<sup>•+</sup> occurs by two ways: the electron transfer from NPG to **1**, Eq. (1) and the reaction of (H)**1d**<sup>•</sup> and surplus NPG, Eq. (7), leading to metastable (H)**1**<sup>-</sup>, which eventually will regenerate product **1** in a similar way to that which we reported for 3-phenyl-quinoxalin-2-ones and amines (19,20).



It is interesting to notice that the initial growth of the ground depletion at 340 nm has the same profile of the NPG<sup>•+</sup> growth, suggesting that the reaction of **1d** with the PhNHCH<sub>2</sub><sup>•</sup> is able to generate more NPG<sup>•+</sup>, see inset in Fig. 9. After delay times >10  $\mu\text{s}$ , a nearly parallel decay for all the absorptions monitored can be observed. Moreover, the increasing ground depletion at 340 nm which follows after long delay times, strongly suggests a chain radical reaction consuming the ground state 3-methyl-

quinoxalin-2-one by PhNHCH<sub>2</sub>• leading to the products **2** and **3**, Eqs. (3) and (4). For all of the studied substrates **1a–f** a completely analogous flash photolysis behavior was observed. The time-resolved spectroscopic study will be published elsewhere.

Having two ways to generate NPG<sup>•+</sup> and hence two PhNHCH<sub>2</sub>• *via* the reactions of Eqs. (1) and (7) could account for a maximal  $\Phi_{pc} = 2$ , therefore other processes likely involving PhNHCH<sub>2</sub>• and the ground state **1**, probably contribute to the generation of more PhNHCH<sub>2</sub>• radicals. It is a well-known fact that the  $\alpha$ -aminoalkyl radicals are strong one electron reductants (41–44), thus, they might be able to reduce the quinoxalin-2-ones generating the respective radical anions **1**<sup>•–</sup> and a H<sup>+</sup>, Eq. (8), giving origin to (H)**1**•, which is able to oxidize NPG, Eq. (7).



Moreover, the intermediate radicals leading to products **2** and **3** probably are also able to oxidize NPG contributing to the chain reaction.

These preceding reactions may rationalize the almost parallels decays observed for all the transient species at longer times after the laser pulse and the increasing consumption of the ground state 3-methyl-quinoxalin-2-one with [NPG], see inset in Figs. 8 and 9. The electron abstraction of processes 7 and 8 generating PhNHCH<sub>2</sub>• can explain the Hammett correlation with  $\sigma^+$ , being the most electron-withdrawing substituent those which more easily should abstract an electron from PhNHCH<sub>2</sub>• or NPG.

By considering the flash photolysis results, the lack of the reactions in oxygenated samples, the structures of the products, the high photoconsumption quantum yields and the Hammett correlation, which can be explained only by considering a radical chain reaction, a reaction mechanism can be proposed. It should include a photoinduced one electron transfer from NPG to excited triplet quinoxalin-2-ones, <sup>3</sup>**1**, Eq. (1), generating the radical ion pair, which should lead to (H)**1**• and PhNHCH<sub>2</sub>•, Eq. (2), and a competitive hydrogen transfer, Eq. (6), leading to the same radical pair. These radicals can combine in a termination reaction to product **2**, Eq. (3), or initiate the chain propagation reactions of Eqs. (7) and (8). The consumption of two PhNHCH<sub>2</sub>• by reactant **1**, would terminate the radical propagation leading to product **3**, Eq. (4). Other termination steps, explaining the formation of (PhNHCH<sub>2</sub>)<sub>2</sub> and, PhN=CH<sub>2</sub> and PhNHCH<sub>3</sub>, by radical addition or hydrogen transfer, respectively, might also be considered.

## CONCLUSIONS

Photoreaction between the 7-substituted-3-methyl-quinoxalin-2-ones **1a–f** and NPG yielded the expected addition product **2** identified by CI mass spectra. We were not able to find literature reporting quinoxalin-2-ones bearing two substituents in position 3, likely due to an inherent instability of this kind of products. Moreover, our findings show that **2a–f** decomposed during EI mass analyses (70 eV) and likely in contact with silica, precluding their isolation and NMR characterization. Even so, the structure we propose for product **2**, supported by experimental evidence, seems reasonable.

The flash photolysis results presented here provide evidence for almost all of the proposed intermediaries and strongly support a radical chain reaction that consumes the ground state 3-methyl-quinoxalin-2-one derivatives. This reaction should lead to radical addition intermediaries that likely are able to oxidize NPG

contributing to the radical chain reaction. As we stated earlier, the complete flash photolysis study will be published elsewhere.

Surprisingly, what looks like a simple photochemically initiated radical addition reaction leads to the totally unexpected annulation product **3** which were unequivocally characterized in this work. As far as we know, there are no reports of photochemical or radical reactions leading to similar annulations products. On the other hand, the large quinoxalin-2-one photoconsumption quantum yields observed for the F-, H-, CF<sub>3</sub>-, and CN-derivatives, see Table 1, require a chain radical reaction able to generate NPG<sup>•+</sup> and hence PhNHCH<sub>2</sub>•. We propose four possible paths for these radical propagation reaction: (H)**1**• abstracting electrons from NPG, Eq. (7); **1** abstracting electron from PhNHCH<sub>2</sub>•, Eq. (8); and the electron and/or hydrogen abstraction from NPG by the intermediaries addition radicals which leads to products **2** and **3**. Thus, the greater the 3-methyl-quinoxalin-2-one substituent electron-withdrawing power, the more easy should be the electron abstraction from the NPG or PhNHCH<sub>2</sub>• explaining the observed Hammett correlation of photoconsumption yields.

Therefore, photolysis of common reactants widely used as NPG and substituted quinoxalin-2-ones may provide a synthetic way to the unusual, substituted imidazoquinoxalinones **3a–f** that has never been reported.

*Acknowledgements*—We thank Dr. Gordon L. Hug for his careful reading of the manuscript; Prof. Dr. F. Castañeda M. for valuable discussion and advice; thanks are also due to F. Morales from *Del Carpio Analysis* for the tandem MS–MS spectra; and to B. Sepulveda from *CEPEDEQ, U. de Chile* for the CI GC-MS analysis; and to FONDECYT grant 1100121 for the financial support. C. Aliaga acknowledges the FONDECYT grant 3130697.

## SUPPORTING INFORMATION

Additional Supporting Information may be found in the online version of this article:

**Data S1.** <sup>1</sup>H and <sup>13</sup>C NMR and MS for compound **1a–f**; EI MS chromatograms for products **2a–f** and **3a–f**; and <sup>1</sup>H, <sup>13</sup>C NMR 1D and 2D spectra for products **3a** and **e**, can be found at DOI: 10.1111/php.12162

## REFERENCES

- Kamila, S. and E. R. Biehl (2006) Synthetic studies of bioactive quinoxalinones: A facile approach to potent euglycemic and hypolipidemic agents. *Heterocycles* **68**, 1931–1939.
- Olayiwola, G., C. A. Obafemi and F. O. Taiwo (2007) Synthesis and neuropharmacological activity of some quinoxalinone derivatives. *Afr. J. Biotechnol.* **6**, 777–786.
- Gris, J., R. Glisoni, L. Fabian, B. Fernandez and A. G. Moglioni (2008) Synthesis of potential chemotherapeutic quinoxalinone derivatives by biocatalysis or microwave-assisted Hinsberg reaction. *Tetrahedron Lett.* **49**, 1053–1056.
- Li, X., K. H. Yang, W. L. Li and W. F. Xu (2006) Recent advances in the research of quinoxalinone derivatives. *Drug Future* **31**, 979–989.
- Carta, A., S. Piras, G. Loriga and G. Paglietti (2006) Chemistry, biological properties and SAR analysis of quinoxalinones. *Mini-Rev. Med. Chem.* **6**, 1179–1200.
- Patel, M., R. J. McHugh, B. C. Cordova, R. M. Klabe, S. Erickson-Viitanen, G. L. Trainor and J. D. Rodgers (2000) Synthesis and eval-

- uation of quinoxalinones as HIV-1 reverse transcriptase inhibitors. *Abstr. Pap. Am. Chem. Soc.*, **219**, 123.
- Matuszczak, B. and K. Mereiter (1997) Syntheses in the series of pyrazolyl-substituted quinoxalines. *Heterocycles* **45**, 2449–2462.
  - Dudash, J., Y. Z. Zhang, J. B. Moore, R. Look, Y. Liang, M. P. Beavers, B. R. Conway, P. J. Rybczynski and K. T. Demarest (2005) Synthesis and evaluation of 3-anilino-quinoxalinones as glycogen phosphorylase inhibitors. *Bioorg. Med. Chem. Lett.* **15**, 4790–4793.
  - Mori, Y., T. Hirokawa, K. Aoki, H. Satomi, S. Takeda, M. Aburada and K. I. Miyamoto (2008) Structure activity relationships of quinoxalin-2-one derivatives as platelet-derived growth factor-beta receptor (PDGF beta R) inhibitors, derived from molecular modeling. *Chem. Pharm. Bull.* **56**, 682–687.
  - Aoki, K., J. Koseki, S. Takeda, M. Aburada and K. Miyamoto (2007) Convenient synthetic method for 3-(3-substituted indol-2-yl) quinoxalin-2-ones as VEGF inhibitor. *Chem. Pharm. Bull.* **55**, 922–925.
  - Willardsen, J. A., D. A. Dudley, W. L. Cody, L. G. Chi, T. B. McClanahan, T. E. Mertz, R. E. Potoczak, L. S. Narasimhan, D. R. Holland, S. T. Rapundalo and J. J. Edmunds (2004) Design, synthesis, and biological activity of potent and selective inhibitors of blood coagulation factor Xa. *J. Med. Chem.* **47**, 4089–4099.
  - Kawanishi, N., T. Sugimoto, J. Shibata, K. Nakamura, K. Masutani, M. Ikuta and H. Hirai (2006) Structure-based drug design of a highly potent CDK1,2,4,6 inhibitor with novel macrocyclic quinoxalin-2-one structure. *Bioorg. Med. Chem. Lett.* **16**, 5122–5126.
  - Kucybala, Z. and J. Paczkowski (1999) 3-Benzoyl-7-diethylamino-5-methyl-1-phenyl-1H-quinoxalin-2-one: An effective dyeing photo-initiator for free radical polymerization. *J. Photochem. Photobiol. A-Chem.* **128**, 135–138.
  - Nishio, T. (1990) Photochemical-reactions of quinoxalin-2-ones and related-compounds. *J. Chem. Soc. Perk. T 1*, 565–570.
  - Nishio, T. (1984) The (2+2) photocycloaddition of the carbon-nitrogen double bond of quinoxalin-2(1H)-ones to electron-deficient olefins. *J. Org. Chem.* **49**, 827–832.
  - Nishio, T. and Y. Omote (1985) Photocycloaddition reactions of 1,4-benzoxazin-2-ones and electron-poor olefins. *J. Org. Chem.* **50**, 1370–1373.
  - Nishio, T. (1992) Photocycloaddition of quinoxaline-2(1h)-thiones to alkenes. *Helv. Chim. Acta* **75**, 487–492.
  - Nishio, T. and C. Kashima (1995) Photochemistry of nitrogen-containing six-membered heterocycles conjugated with carbonyl. *Rev. Heteroatom Chem.* **13**, 149–177.
  - de la Fuente, J. R., A. Cañete, A. L. Zanocco, C. Saitz and C. Jullian (2000) Formal hydride transfer mechanism for photoreduction of 3-phenylquinoxalin-2-ones by amines. Association of 3-phenylquinoxalin-2-one with aliphatic amines. *J. Org. Chem.* **65**, 7949–7958.
  - De la Fuente, J. R., A. Cañete, C. Saitz and C. Jullian (2002) Photoreduction of 3-phenylquinoxalin-2-ones by amines: Transient-absorption and semiempirical quantum-chemical studies. *J. Phys. Chem. A* **106**, 7113–7120.
  - De la Fuente, J. R., C. Jullian, C. Saitz, E. Sobarzo-Sanchez, V. Neira, C. Gonzalez, R. Lopez and H. Pessoa-Mahana (2004) Photoreduction of oxoisoaporphines. Another example of a formal hydride-transfer mechanism. *Photochem. Photobiol. Sci.* **3**, 194–199.
  - De la Fuente, J. R., C. Jullian, C. Saitz, V. Neira, O. Poblete and E. Sobarzo-Sanchez (2005) Unexpected formation of 1-diethylaminobutadiene in photosensitized oxidation of triethylamine induced by 2,3-dihydro-oxoisoaporphine dyes. A H-1 NMR and isotopic exchange study. *J. Org. Chem.* **70**, 8712–8716.
  - De la Fuente, J. R., V. Neira, C. Saitz, C. Jullian and E. Sobarzo-Sanchez (2005) Photoreduction of oxoisoaporphine dyes by amines: Transient-absorption and semiempirical quantum-chemical studies. *J. Phys. Chem. A* **109**, 5897–5904.
  - De la Fuente, J. R., G. Kciuk, E. Sobarzo-Sanchez and K. Bobrowski (2008) Transient phenomena in the pulse radiolysis of oxoisoaporphine derivatives in acetonitrile. *J. Phys. Chem. A* **112**, 10168–10177.
  - De la Fuente, J. R., C. Aliaga, C. Poblete, G. Zapata, C. Jullian, C. Saitz, A. Cañete, G. Kciuk, E. Sobarzo-Sanchez and K. Bobrowski (2009) Photoreduction of oxoisoaporphines by amines: Laser flash and steady-State photolysis, pulse radiolysis, and TD-DFT studies. *J. Phys. Chem. A* **113**, 7737–7747.
  - Canle, M., J. A. Santaballa and S. Steenken (1999) Photo- and radiation-chemical generation and thermodynamic properties of the aminium and aminyl radicals derived from N-phenylglycine and (N-chloro, N-phenyl)glycine in aqueous solution: Evidence for a new photoionization mechanism for aromatic amines. *Chem.-Eur. J.* **5**, 1192–1201.
  - Bonifacic, M., I. Stefanic, G. L. Hug, D. A. Armstrong and K.-D. Asmus (1998) Glycine decarboxylation: The free radical mechanism. *J. Am. Chem. Soc.* **120**, 9930–9940.
  - Lalevee, J., B. Graff, X. Allonas and J. P. Fouassier (2007) Aminooalkyl radicals: Direct observation and reactivity toward oxygen, 2,2,6,6-tetramethylpiperidine-N-oxyl, and methyl acrylate. *J. Phys. Chem. A* **111**, 6991–6998.
  - Boule, P. and J. F. Pilichowski (1993) Comments about the use of aberchrome (Tm)-540 in chemical actinometry. *J. Photochem. Photobiol. A* **71**, 51–53.
  - Hansch, C., A. Leo and R. W. Taft (1991) A survey of hammett substituent constants and resonance and field parameters. *Chem. Rev.* **91**, 165–195.
  - Zavitsas, A. A. and G. M. Hanna (1975) Reactions of undecyl radicals with substituted toluenes. *J. Org. Chem.* **40**, 3782–3783.
  - Acton, A., A. D. Allen, A. V. Fedorov, H. Henry-Riyad and T. T. Tidwell (2006) Aminooxyl radical addition to arylketenes. *J. Phys. Org. Chem.* **19**, 841–846.
  - Pryor, W. A., F. Y. Tang, R. H. Tang and D. F. Church (1982) Chemistry of the tert-butyl radical: Polar character, rho. Value for reaction with toluenes, and the effect of radical polarity on the ratio of benzylic hydrogen abstraction to addition to aromatic rings. *J. Am. Chem. Soc.* **104**, 2885–2891.
  - Pryor, W. A., W. H. Davis and J. P. Stanley (1973) Polar effects in radical reactions. II. Positive rho. for the reaction of tert-butyl radicals with substituted toluenes. *J. Am. Chem. Soc.* **95**, 4754–4756.
  - Davis, W. H. and W. A. Pryor (1977) Polar effects in radical reactions. 7. Positive rho. values for the reactions of isopropyl and tert-butyl radicals with substituted toluenes. *J. Am. Chem. Soc.* **99**, 6365–6372.
  - Ito, O. and M. Matsuda (1982) Determination of addition rates of thyl radicals to vinyl monomers by means of flash photolysis. 8. Polar effect in addition rates of substituted benzenethiyl radicals to alpha-methylstyrene determined by flash photolysis. *J. Org. Chem.* **47**, 2261–2264.
  - Ito, O. and M. Matsuda (1981) Evaluation of addition rates of thyl radicals to vinyl monomers by flash photolysis. 3. Polar effect in addition reactions of substituted benzenethiyl radicals. *J. Am. Chem. Soc.* **103**, 5871–5874.
  - Ikedo, S. and S. Murata (2002) Photolysis of N-phenylglycines sensitized by polycyclic aromatic hydrocarbons - Effects of sensitizers and substituent groups and application to photopolymerization. *J. Photochem. Photobiol. A* **149**, 121–130.
  - Ikedo, S., S. Murata, K. Ishii and H. Hamaguchi (2000) Mechanistic studies of the pyrene-sensitized photodecomposition of N-phenylglycine: Acceleration of the photodecomposition by the addition of an electron acceptor. *B. Chem. Soc. Jpn.* **73**, 2783–2792.
  - Liu, W. Z. and F. G. Bordwell (1996) Gas-phase and solution-phase homolytic bond dissociation energies of H-N+ bonds in the conjugate acids of nitrogen bases. *J. Org. Chem.* **61**, 4778–4783.
  - Wayner, D. D. M., D. J. McPhee and D. Griller (1988) Oxidation and reduction potentials of transient free radicals. *J. Am. Chem. Soc.* **110**, 132–137.
  - Hiller, K.-O. and K.-D. Asmus (1983) Formation and reduction reactions of alpha-amino radicals derived from methionine and its derivatives in aqueous solutions. *J. Phys. Chem.* **87**, 3682–3688.
  - Mönig, J., R. Chapman and K.-D. Asmus (1985) Effect of the protonation state of the amino group on the ·OH radical induced decarboxylation of amino acids in aqueous solution. *J. Phys. Chem.* **89**, 3139–3144.
  - Bobrowski, K., B. Marciniak and G. L. Hug (1992) 4-Carboxybenzophenone-sensitized photooxidation of sulfur-containing amino acids. Nanosecond laser flash photolysis and pulse radiolysis studies. *J. Am. Chem. Soc.* **114**, 10279–10288.